Chapter 7

Crystallization, data collection and X-ray structural studies of WCI mutant N14T

7.1. Crystallization of N14T

Since WCI and its mutants (N14K and N14D) were crystallized using ammonium sulfate (AMS) as precipitant, the initial crystallization trials of N14T were attempted with AMS. Varying concentrations of AMS were tried with a protein concentration of 16 mg/ml (in 50 mM Tris, 100 mM NaCl, pH 8.0), but no useful crystal was obtained. Hampton Screen and other precipitants like PEG 4K, 6K and 8K were also tried, mainly using hanging drop vapor diffusion method at two different temperatures, 4°C and 20°C and finally the drops with 12% PEG 4K, set at 20°C, indicated the initiation of crystallization (Fig 7.1.a) The needle like crystals were then fished out from the drop, dissolved in the above mentioned buffer and checked in a 15% SDS-polyacrylamide gel (Fig. 7.1.b; lane C). The protein sample, used for crystallization, was also loaded in another lane (Fig. 7.1.b; lane P). Lanes C and P match well indicating that the protein molecules in the crystals are of same molecular weight as that of mutant protein N14T and no degradation has occurred during crystallization.

To improve the crystal quality for X-ray diffraction studies, fine grids around this crystallization condition were tried with varying PEG concentrations and pH and the best crystals were obtained in a droplet of 6μl, where 3μl of protein was mixed with 3μl of 5% PEG 4K in 50 mM Tris, 100 mM NaCl, pH 8.0, equilibrated against the reservoir, containing 40% PEG 4K in the same buffer. Thin plate shaped crystals were grown to a maximum size of 0.4 x 0.2 x 0.1 mm (Fig. 7.2 b) in about 12 days and used for subsequent data collection

7.2. Data collection of N14T

X-ray data for N14T were collected upto 3.0 Å resolution using 30cm MAR research image-plate detector with copper Kα radiation from Rigaku RU-200B rotating-anode generator, equipped with Osmic MaxFlux confocal optics, running at 50kV and 90mA. Crystals, grown in presence of PEG 4K, were fished out from the crystallization drops and straightway flash-frozen in a stream of nitrogen (Oxford cryo-system) at 100K.

A total of 75 frames were collected with a crystal to detector distance of 140 mm with an exposure time of 6 minutes and oscillation range of 1°. The data were processed using the programs DENZO and SCALEPACK from the HKL program package (Otwinowski and Minor, 1997). Evaluation of the crystal packing parameters for N14T indicated that the lattice can accommodate two molecules in the asymmetric unit with a V_M ($Å^3$/Da) value (Matthews, 1968) of 1.83 and solvent content of 31%. The data collection and processing parameters are listed in Table 7.1.

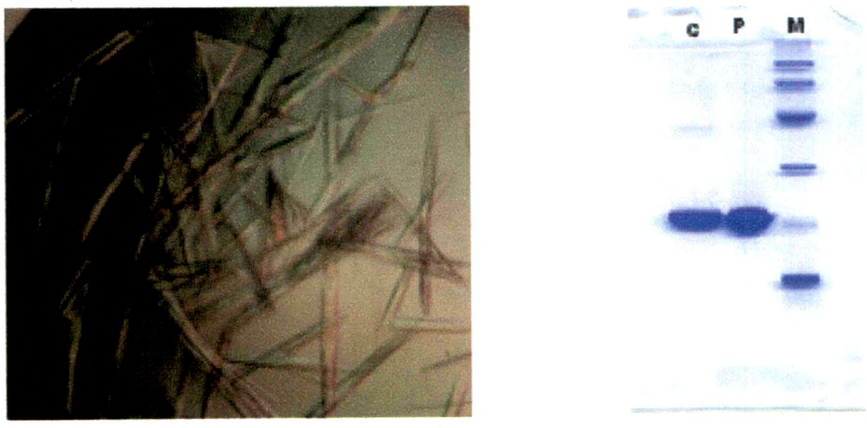

(a) (b)

Figure 7.1. (a) Crystals of N14T, grown in PEG 4K at 20°C; (b) a 15% SDS-polyacrylamide gel; lane C shows the band of dissolved crystals and lane P showed the bands of protein sample used for crystallization.

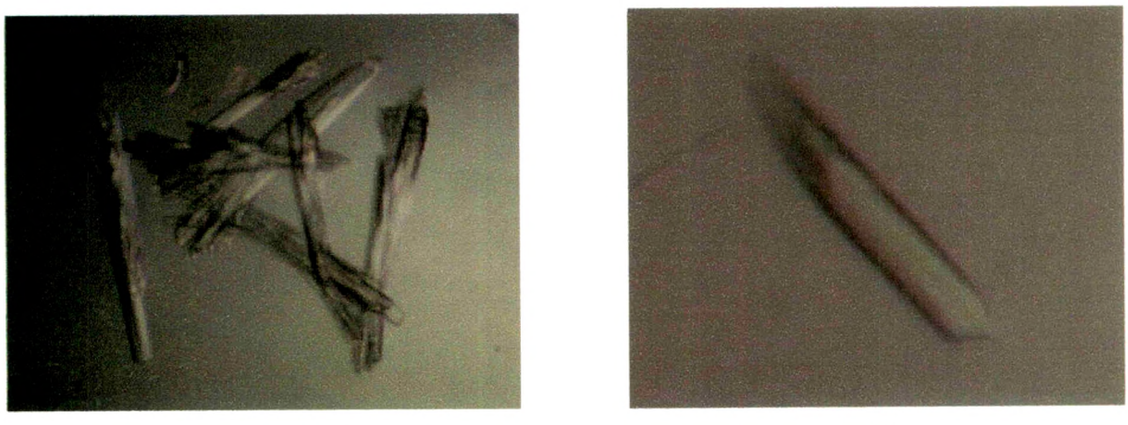

(a) (b)

Figure 7.2. Stages of improvements of N14T crystals, grown in PEG 4K at 20°C

Table 7.1. Data collections and crystal statistics for N14T

Space group	$P2_12_12_1$
Unit cell parameters	a=34.103; b=71.288; c=129.644
Mosaicity	0.8
Mathews coefficient	1.83
Solvent content %)	31%
No. of molecules in asymmetric unit	2
Resolution range (Å)	10-3.0
No. of observations	23,416
No. of unique reflections	6,605
R merge (%)	
Overall	14.2
Last shell	43.3
R_{sym} (%)	11.6
I/SigI	8.2
Completeness (%)	
Overall	99.1
Last shell	98.6
Wilson B-factor (Å2)	25.5

7.3. Structure determination and refinement

Molecular replacement calculations for N14T was done using AMoRe (CCP4) with the data between 10-3.5 Å. Initially the coordinates of recombinant WCI (PDB code:1EYL) was taken as starting model, excluding only the three extra N-terminal residues, but no clear solution was obtained. Then we started deleting the flexible loops and other poorly defined regions 1-3, 63-66, 137-142, 163-165, 174-180 from the starting model and the remaining portions were converted to poly ALA model This modified model gave the solutions in AMoRe with a corelation coefficient of 44.1% and R factor of 47.3%. The two moleculaes were placed in the asymmetric unit applying the rotation and translation functions, obtained from AMoRe.

Before starting the refinement, 5% of the reflections were randomly chosen by the program 'make_cv.inp' of CNS for R_{free} calculations (Brunger, 1992). Initially, a rigid body refinement was performed using CNS. A σ_A weighted $2F_o$-F_c electron density map was calculated (Read, 1986) at this stage to verify the placements of the molecules in the asymmetric unit. Next set of refinement and model building were performed by CNS (Brünger *et al.*, 1998) and 'O' version 7.2 (Jones *et al.*, 1991) respectively and the progress of refinement was monitored by checking the R and free R values.

After three cycles of main-chain fitting and subsequent positional refinement, the R factor dropped to 39.2% (R_{free} 42.2%). At this stage, the side chains of the residues from core region became unambiguous and they were incorporated accordingly. After another two cycles of model building and refinement R factor dropped to 36.1% (R_{free} 39.2%) and some of the excluded regions including N and C terminus started appering in the newly calculated electron density map. Gradual incorporation of side chain and the regions, which were omitted in the model, further dropped the R factor to 33.3% (R_{free} 36.1%). A several cycles of model buildings

followed by simulated annealing, positional refinement and grouped temperature factore (B group) refinement dropped the R factor to 27.2% (R_{free} 32.2%). At the last stage of refinement, the side chain of Thr was incorporated in the already developed electron density at the 14th position (Fig. 7.3). Some more minor corrections were done in the model. After final cycle of refinement, the R factor dropped to 26.5% (R_{free} 31.3%). for 1355 protein atoms. The model quality is judged which shows the rmsd of bond lengths and bond angles from ideal values as 0.029 Å and 2.6° respectively.

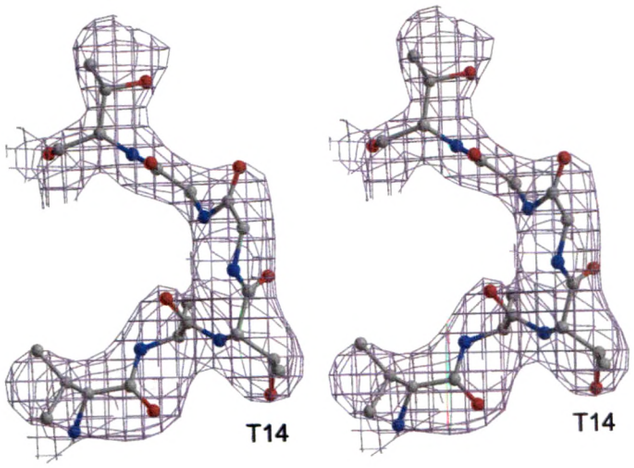

Figure 7.3. Sterepscopic representation of the 2Fo-Fc electron density map (contoured at 1.2 σ) around the region Val12-Thr17, which includes the mutation site Thr14.

7.4. Structure analysis

The objective of crystal structure determination of N14T was to establish the observations that we obtained from MD simulations (Dasgupta *et al.*, 2003) at the experimental level. For this purpose it was necessary to compare the crystal structure with the corresponding simulated structure. At first, the dihedral angles of the reactive site loop region of N14T are calculated and compared with the corresponding values of rWCI and the simulated average structure of N14T (Table 7.2), which shows that the reactive site loop region of N14T falls within the range of canonical conformation. The reactive site loop (P3-P3′) obtained from the crystal structure of N14T superposes on the simulated structure of N14T with an rmsd value of 0.7Å (Fig. 7 4), which indicates that the reactive site loop region of the crystal structure resembles substantially with the simulated structure. Moreover, the side chain orientation of Thr14 in the crystal structure is also similar to that of the simulated structure (Fig. 7.4). In the crystal structure, the side chain OG atom of Thr14 forms hydrogen bond (3.25 Å) with carbonyl O atoms of Ser66 (P1′) whereas main chain N atom of Thr14 forms hydrogen bond (3.05 Å) with P2′ carbonyl O, providing stability to the C terminal part of the scissile bond. Similar hydrogen bonding pattern was observed in the reactive site loop region of the simulated structure N14T (Fig. 5.5.a; Chapter 5).

Table 7.2. Comparison of dihedral angle values (P3-P3′) of crystal structures with simulated structures for rWCI and N14T

	P3 (ϕ/φ)	P2 (ϕ/φ)	P1 (ϕ/φ)	P1′ (ϕ/φ)	P2′ (ϕ/φ)	P3′ (ϕ/φ)
WCI	-71.3/-17.5	-97.8/168.0	-82.4/-9.1	-55.4/158.4	-73.7/-29.2	-119.6/-174.2
WCI (MD)	-64.7/-30.8	-75.0/-173.0	-108.5/37	-75.4/140.8	-57.8/-52.7	-99.8/-173.7
N14T	-88.7/-2.8	-113.4/129.2	-69.7/28.8	-101.1/172	-74.8/0.3	-150/143.5
N14T (MD)	-55.6/-58.6	-77/157.3	-93.2/37.6	-68.6/163.6	-83.4/-31.3	-124.8/133.5

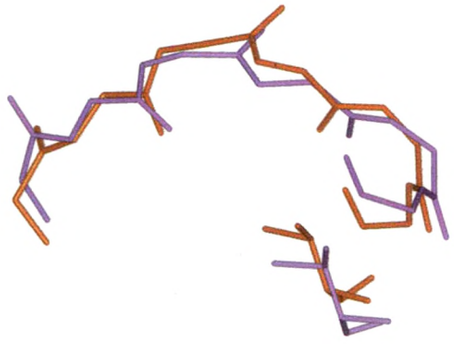

Figure 7.4. Superposition of the reactive site loop (P3-P3′) of the crystal structure of N14T (violet) on that of the simulated average structure (red).

Therefore the results obtained from the crystal structure analysis matches well with the observations, obtained from MD simulations. The biochemical study of inhibition of chymotrypsin by N14T is also in accordance with the conclusion of MD results. The small differences in dihedral angles between the simulated and crystal structures may be attributed to the involvement of the reactive site loop in the crystal packing (the solvent content is only 31%). Same orders of differences, either in rmsd or in dihedral angles, are observed between simulated and crystal structures of WCI. Considering these facts, it can be concluded that the reactive site loop of N14T agrees well with the canonical conformation.